Opto-Electronic Science

Supplementary information

2024, Vol. 3, No.

DOI: 10.29026/oes.2024.230035

Supercritical metalens at h-line for high-resolution direct laser writing

Jichao Fu[1†], Mengting Jiang[1†], Zeng Wang[1], Yi Fan Chen[1], Yuanda Liu[1], Qing Yang Steve Wu[1], Ai Jia Sim[1], Jiang Wang[1,2], Mingxi Chen[1], Ziyu Wang[1], Jie Deng[1], Xiao Song Eric Tang[1], Kun Huang[3], Hong Liu[1] and Jinghua Teng[1*]

[1]Institute of Materials Research and Engineering (IMRE), Agency for Science, Technology and Research (A*STAR), 2 Fusionopolis Way, Innovis #08-03, Singapore 138634, Singapore; [2]School of Microelectronics, Hefei University of Technology, Hefei, Anhui 230009, China; [3]Department of Optics and Optical Engineering, University of Science and Technology of China, Hefei, Anhui 230026, China.

[†]These authors contributed equally to this work.

*Correspondence: JH Teng, E-mail: jh-teng@imre.a-star.edu.sg

This file includes:

Supplementary information for this paper is available at https://doi.org/10.29026/oes.2024.230035

Section 1: Vectorial diffraction formula

Suppose the source plane is $\boldsymbol{x}' = (x', y', z' = 0)$ and target plane is $\boldsymbol{x} = (x, y, z)$, and the time harmonic factor of the fields is $\exp(-\mathrm{i}\omega t)$.

Then the electromagnetic fields at the target plane can be calculated from the fields at the source plane[S1], as

$$\boldsymbol{E}(\boldsymbol{x}) = \frac{1}{4\pi}\iint_{\Sigma}\left[\mathrm{i}\omega\left(\widehat{\boldsymbol{N}}\times\boldsymbol{B}_{\Sigma}(\boldsymbol{x}')\right)G + \left(\widehat{\boldsymbol{N}}\times\boldsymbol{E}_{\Sigma}(\boldsymbol{x}')\right)\times\nabla'G + \left(\widehat{\boldsymbol{N}}\cdot\boldsymbol{E}_{\Sigma}(\boldsymbol{x}')\right)\nabla'G\right]\mathrm{d}^2\boldsymbol{x}' ,$$

where $\boldsymbol{R} = \boldsymbol{x} - \boldsymbol{x}' = \begin{pmatrix} x - x' \\ y - y' \\ z - z' \end{pmatrix}$, is the position vector; $\widehat{\boldsymbol{N}} = \boldsymbol{z} = \widehat{\boldsymbol{k}}_{\Sigma} = \begin{pmatrix} 0 \\ 0 \\ 1 \end{pmatrix}$, is the normal direction of the source plane, $k = \omega\sqrt{\mu\varepsilon}$ the wavevector (ω the angular frequency, μ the permeability and ε the permittivity), $\boldsymbol{E}_{\Sigma}(x') = \begin{pmatrix} E'_x \\ E'_y \\ E'_z \end{pmatrix}$ the electric field at the source plane (as the supercritical lenses are located near the focal position of the conventional lens, E'_z is nearly zero), $\boldsymbol{B}_{\Sigma}(x') = \sqrt{\mu\varepsilon}k\times\boldsymbol{E}_{\Sigma}(x') = \frac{k}{\omega}\begin{pmatrix} -E'_y \\ E'_x \\ 0 \end{pmatrix}$ the magnetic flux density at the source plane, $G = \frac{\exp(\mathrm{i}kR)}{R}$, $\nabla'G = -\frac{\exp(\mathrm{i}kR)(\mathrm{i}kR - 1)}{R^3}\begin{pmatrix} x - x' \\ y - y' \\ z - z' \end{pmatrix}$. After simplification, the three components of $\boldsymbol{E}(\boldsymbol{x})$ can be written explicitly as:

$$\begin{pmatrix} E_x \\ E_y \\ E_z \end{pmatrix} = -\frac{1}{4\pi}\iint_{\Sigma}\left\{\mathrm{i}kG\begin{pmatrix} E'_x \\ E'_y \\ 0 \end{pmatrix} + G\left(\frac{\mathrm{i}k}{R} - \frac{1}{R^2}\right)\begin{pmatrix} z\cdot E'_x \\ z\cdot E'_y \\ -E'_x(x - x') - E'_y(y - y') \end{pmatrix}\right\}\mathrm{d}^2\boldsymbol{x}'$$

Section 2: The efficiencies of the ideal lens, FZL and SCLs

By "ideal lens", we mean a lens with a phase profile following Fermat's principle. Its intensity at the focal spot can be estimated analytically as below.

The incidence beam is a Gaussian beam with a waist radius of 25 μm, and the intensity at its central position (x = 0, y = 0, z = 0) is assumed to be 1. Then the input electric field intensity is $I_0 = \exp(-2r^2/w_0^2)$, where $r = \sqrt{x^2 + y^2}$ is the radial position and w_0 is the waist radius. The input power upon the metalens is

$$P_0 = \frac{1}{2\eta_0}\int_0^{25\ \mu\mathrm{m}} I_0 2\pi r\mathrm{d}r,$$

where η_0 is the wave impendence in the air.

The focal spot by this ideal lens is a diffraction-limited Airy spot ($FWHM$ = 0.5 × λ/NA = 452.8 nm), with an intensity distribution of,

$$I_1 = A\left[\frac{2J_1(sr)}{sr}\right]^2 ,$$

where, A is the intensity enhancement factor to be determined, J_1 is the Bessel function of the first kind of order one, and $s = \frac{1.616}{FWHM/2}$ is the scaling factor to make $I_1 = 0.5A$ at $x = FWHM/2$. The power through the focal plane is

$$P_1 = \frac{D(\theta)}{2\eta_0}\int_0^{R_1} I_1 2\pi r\mathrm{d}r ,$$

where R_1, the upper limit of integer, can be put as 5 times of the FWHM here to include most of the power, $D(\theta)$ is a correcting factor considering that the focusing beam is not perpendicular to the focal plane but expanding transversally, and θ is the half-angle of the maximum cone of light. In the air, $NA = \sin\theta$, $\cos\theta = \sqrt{1 - \sin^2\theta} = \sqrt{1 - NA^2}$. The reasonable range of $D(\theta)$ is from $\cos\theta$ to 1. From the principle of energy conversion, $P_0 = P_1$, and immediately, we can get that A should be between 3595 and 4019. Using the vectorial diffraction formula, the value of enhancement factor, A, of the ideal lens is calculated to be 4031, which corresponds quite well with the analytically calculated value.

The maximum intensities at the focal spots are measured to be 349, 134 and 123 times of the maximum intensity of the incident beam, for the FZL, SCL05 and SCL10, respectively, and they are calculated to be 616, 250 and 188 times, respectively, by the vectorial diffraction formula. As the maximum intensity is a critical figure-of-merit in lithography, the efficiency is defined here as the ratio of the maximum intensity at the focal spot of a metalens and that of the reference ideal lens. Then the efficiencies of these three metalenses are 8.7%, 3.3% and 3.1% in experiment, and 15.3%, 6.2% and 4.7% in theory.

We note that if more types of units or units with larger phase differences are adopted, the efficiency can be further improved. For example, AlN pillars with a height of 375 nm and diameters of 60 and 150 nm will have a phase difference of π, and the efficiency of an FZL made from such AlN pillars can be increased to 1184/4031 = 29.4%. Metalenses constructed from units of more types and larger phase differences are preferable in efficiency, while a significantly simplified lens, such as the SCLs here constructed from imperfect units, can still be quite useful in many demanding applications.

Section 3: The performance of the FZL with other possible selections of units "0" and "1"

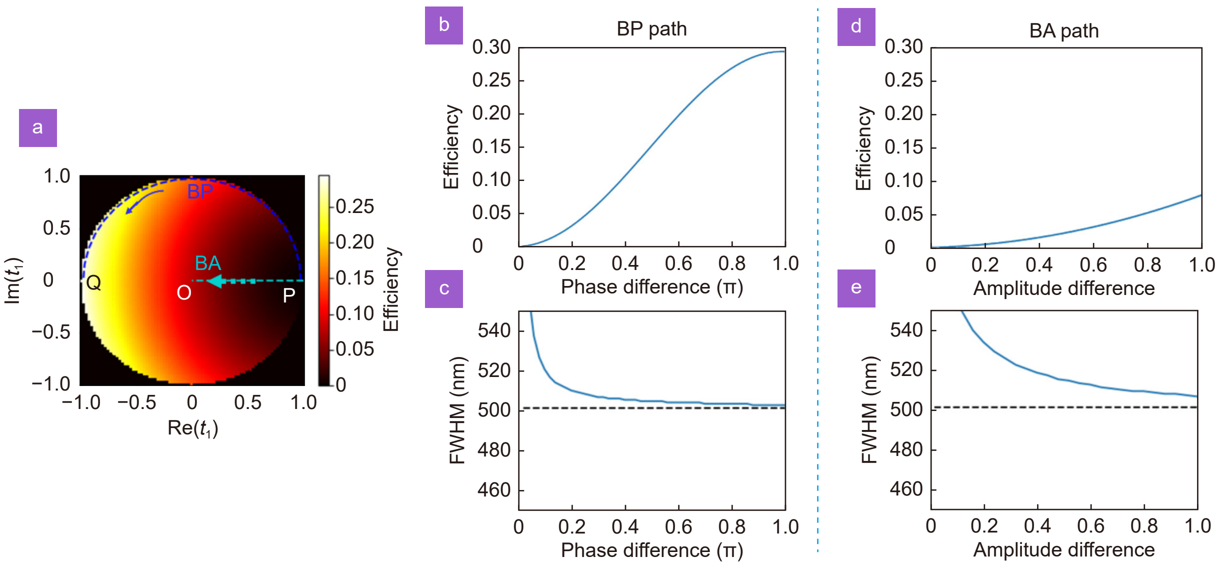

Fig. S1 | The performance of the binary FZL with other possible units "0" and "1". (**a**) The efficiency of the binary FZL with a fixed unit "0" (t_0 = 1) and a unit "1" within (or on) the unit circle on the complex plane of transmission coefficient. The horizontal and vertical axes are the real and imaginary parts of the transmission coefficient of the permitted unit "1", respectively. (**b**, **c**) The change of efficiency (b) and FWHM (c) of the FZL when the unit "1" evolves from point P (t = 1) to point Q (t = −1) through the binary phase (BP) path in (a). (**d**, **e**) The change of efficiency (d) and FWHM (e) of the FZL when the unit "1" evolves from point P to point O (t = 0) through the binary amplitude (BA) path in (a).

Section 4: The FWHMs of the metalenses with different incidence beam sizes

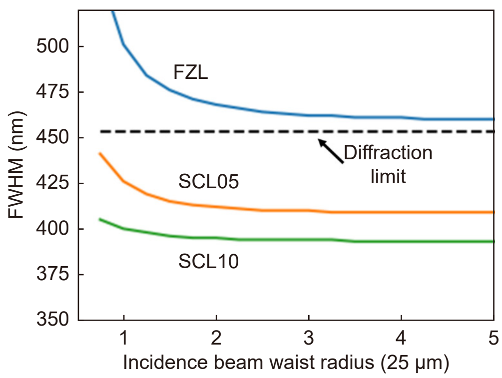

Fig. S2 | FWHMs of the metalenses (FZL, SCL05, and SCL10) when the waist radius of the incidence Gaussian beam changes. The FWHMs of SCL05 and SCL10 are always smaller than the diffraction limit by around 50 nm, while the FWHM of the FZL is always larger than the diffraction limit and only with much larger beam size can it approach the diffraction limit of 452.8 nm.

Section 5: Extended focus in SCL10

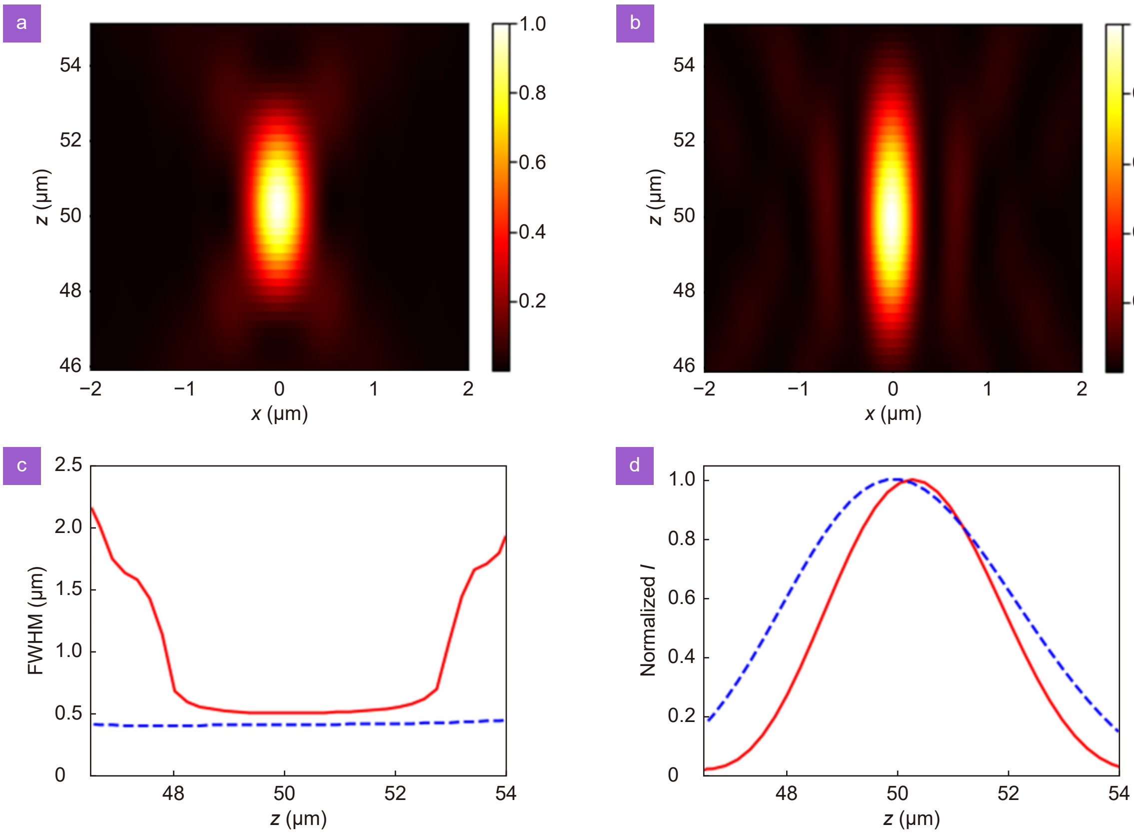

Fig. S3 | Characteristics of focusing pattern and depth of focus of FZL and SCL10. (**a**, **b**) Focusing patterns of FZL (a) and SCL10 (b) in a larger *z* range. (**c**, **d**) The FWHM (c) and normalized intensity (d) along *z* of FZL (red solid line) and SCL10 (blue dashed line).

Section 6: Grating patterns with smaller pitches

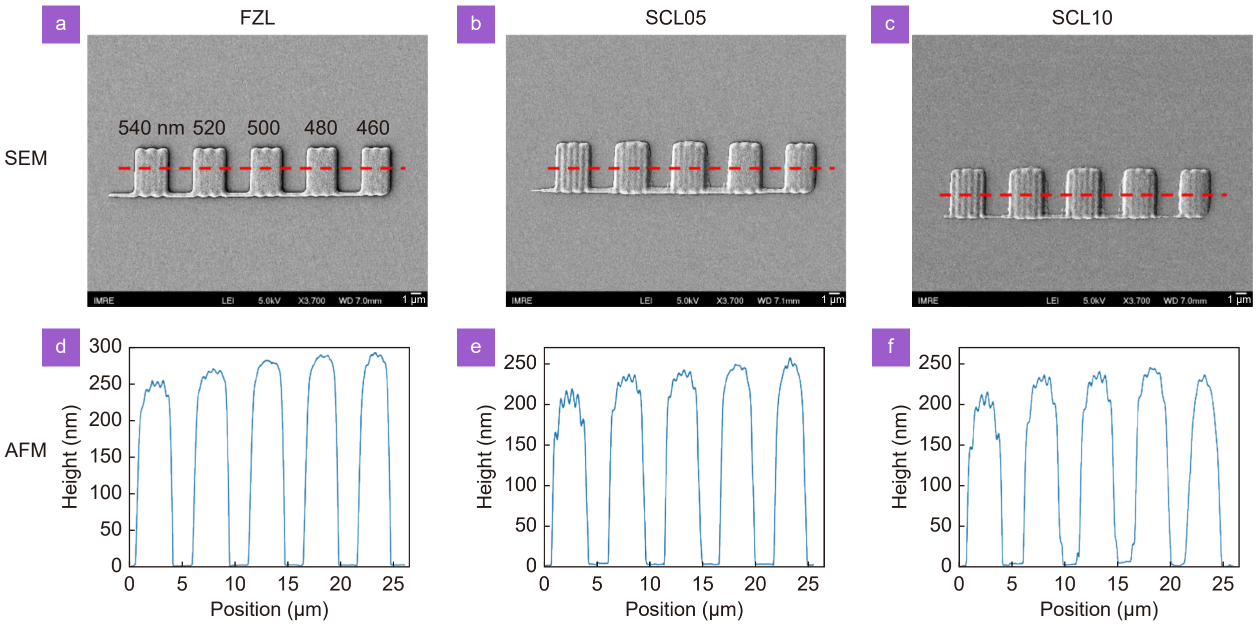

Fig. S4 | Grating patterns generated by the FZL- and SCL-based DLW. (**a**–**c**) SEM images of the grating patterns, from left to right, with pitches of 540, 520, 500, 480 and 460 nm and a length of 4 μm written by the FZL (a), SCL05 (b) and SCL10 (c). (**d**–**f**) Measured height information by AFM (Atomic force microscopy) along the positions indicated by the red dashed lines in (a–c).

Section 7: High-magnification SEM images of the lithography patterns by SCL05

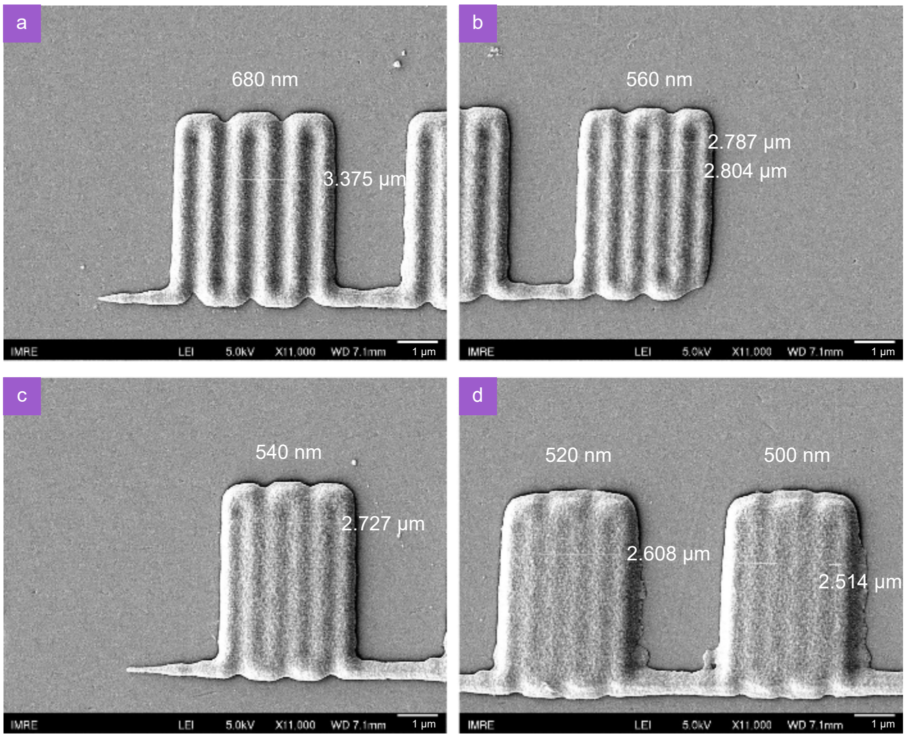

Fig. S5 | High-magnification SEM images of the lithography patterns written by SCL05. (**a**) The group with a pitch of 680 nm. (**b**) The group with a pitch of 560 nm. (**c**) The group with a pitch of 540 nm. (**d**) The groups with a pitch of 520 nm and 500 nm, respectively. The measured distance between the leftmost and rightmost lines (equal to 5 pitches) is labelled in each group.

References

S1. Kim J, Wang Y, Zhang X. Calculation of vectorial diffraction in optical systems. *J Opt Soc Am A* **35**, 526–535 (2018).